

ECOLOGY LETTERS

Predictability in community dynamics

Journal:	<i>Ecology Letters</i>
Manuscript ID	ELE-01028-2016.R1
Manuscript Type:	Ideas and Perspectives
Date Submitted by the Author:	n/a
Complete List of Authors:	Blonder, Benjamin; University of Oxford, Environmental Change Institute Moulton, Derek; University of Oxford, Mathematical Institute Blois, Jessica; University of California, Merced, Life and Environmental Sciences Enquist, Brian; University of Arizona, Ecology and Evolutionary Biology Graae, Bente; Norwegian University of Science and Technology, Department of Biology Macias-Fauria, Marc; University of Oxford, Zoology McGill, Brian; University of Maine, School of Biology Nogu��, Sandra; University of Southampton Ordonez, Alejandro; Aarhus University, Department of Bioscience Sandel, Brody; Aarhus Universitet Svenning, Jens-Christian; Aarhus University , Department of Bioscience
Key Words:	disequilibrium, lag, alternate states, community climate, community assembly, memory effects, hysteresis, state number

1		
2		
3	1	Title
4		
5	2	Predictability in community dynamics
6		
7		
8	3	
9		
10	4	Running title
11		
12		
13	5	Predictability in community dynamics
14		
15	6	
16		
17	7	Type of article
18		
19		
20	8	Ideas and perspectives
21		
22	9	
23		
24	10	Authors
25		
26		
27	11	Benjamin Blonder ^{1,2,*}
28		
29	12	Derek E. Moulton ³
30		
31		
32	13	Jessica Blois ⁴
33		
34	14	Brian J. Enquist ⁵
35		
36		
37	15	Bente J. Graae ²
38		
39	16	Marc Macias Fauria ¹
40		
41	17	Brian McGill ⁶
42		
43		
44	18	Sandra Nogué ⁷
45		
46	19	Alejandro Ordonez ⁸
47		
48		
49	20	Brody Sandel ⁸
50		
51	21	Jens-Christian Svenning ⁸
52		
53	22	
54		
55	23	Affiliations
56		
57		
58		
59		
60		

1
2
3 24 1: Environmental Change Institute, School of Geography and the Environment, University of
4
5
6 25 Oxford, Oxford OX1 3QY, United Kingdom
7

8 26 2: Department of Biology, Norwegian University of Science and Technology, Trondheim, N-
9
10 27 7490 Norway
11

12
13 28 3: Mathematical Institute, University of Oxford, Oxford, OX2 6GG, United Kingdom
14

15 29 4: School of Natural Sciences, University of California – Merced, Merced, California 95343,
16
17 30 United States of America
18

19
20 31 5: Department of Ecology and Evolutionary Biology, University of Arizona, Tucson, Arizona,
21
22 32 85721, USA
23

24 33 6: School of Biology and Ecology, University of Maine, Orono, Maine 04469, USA
25

26
27 34 7: Department of Geography and the Environment, University of Southampton, Southampton,
28
29 35 SO17 1BJ, United Kingdom
30

31 36 8: Section for Biodiversity & Ecoinformatics, Department of Bioscience, Aarhus University,
32
33 37 Aarhus C, DK-8000 Denmark
34

35
36 38
37
38 39 * Corresponding author: email bblonder@gmail.com, phone +44 7599082123, address
40

41 40 Environmental Change Institute, South Parks Road, Oxford, OX1 3QY, United Kingdom
42

43 41
44

45 42
46
47
48
49
50
51
52
53
54
55
56
57
58
59
60

1
2
3
4
5
6
7
8
9
10
11
12
13
14
15
16
17
18
19
20
21
22
23
24
25
26
27
28
29
30
31
32
33
34
35
36
37
38
39
40
41
42
43
44
45
46
47
48
49
50
51
52
53
54
55
56
57
58
59
60

Key words

Disequilibrium, lag, community response diagram, alternate states, chaos, community climate, community assembly, climate change, hysteresis, memory effects

Author contributions

BB conceived the project, carried out analyses, and wrote the manuscript. BB and DM developed theory. All authors provided feedback and contributed to writing. The co-author list was ordered to reflect primary contributions from BB and DM, then ordered alphabetically by last name.

Number of words in abstract: 134

Number of words in main text: 5715

Number of references: 96

Number of figures: 3

Number of boxes: 2

Abstract

The coupling between community composition and climate change spans a gradient from no lags to strong lags. The no-lag hypothesis is the foundation of many ecophysiological models, correlative species distribution modeling, and climate reconstruction approaches. Simple lag hypotheses have become prominent in disequilibrium ecology, proposing that communities track climate change following a fixed function or with a time delay. However more complex dynamics are possible and may lead to memory effects and alternate unstable states. We develop graphical and analytic methods for assessing these scenarios and show that these dynamics can appear in even simple models. The overall implications are that 1) complex community dynamics may be common, and 2) detailed knowledge of past climate change and community states will often be necessary yet sometimes insufficient to make predictions of a community's future state.

1
2
3
4
5
6
7
8
9
10
11
12
13
14
15
16
17
18
19
20
21
22
23
24
25
26
27
28
29
30
31
32
33
34
35
36
37
38
39
40
41
42
43
44
45
46
47
48
49
50
51
52
53
54
55
56
57
58
59
60

Introduction

Understanding how communities respond to climate change is necessary for predictive modeling of global change and for identifying the processes that have shaped contemporary biodiversity patterns. A key aspect is the degree of lag in the response of community composition to contemporary climate conditions. By lag we mean the *amount* the community is out of equilibrium with the observed climate, in either a positive or negative direction. The equilibrium no-lag state of a community should reflect a set of species with climate niche optima close to the observed climate at a given location. However, since climates change over time, a range of transient disequilibrium community states could be achieved, in which the community’s composition is lagged relative to climate.

There are two extreme hypotheses for the magnitude of lags in the response of community composition to climate change. No-lag responses are thought to occur when species respond through local persistence via high niche plasticity or niche adaptation, or rapid extinction at trailing range edges (Hampe & Petit 2005), and/or efficient long-distance dispersal and range expansions at leading range edges. In this case, the community responds instantly to climate change and is in an equilibrium state. Conversely, lagged responses are thought to occur when species have limited dispersal ability, have long persistence times, or when the regional pool does not include more appropriate species (Svenning & Sandel 2013; Blonder *et al.* 2015). In this case, the community is in a transient disequilibrium state that will change both when the climate varies and when the climate does not vary. These two ideas form the conceptual foundation for several large bodies of work and are thought to encompass the range of possible community responses to climate change (Ackerly 2003), with the speed and type of species

response of fundamental interest for predictive modeling and for biodiversity conservation (Nicotra *et al.* 2010; Hoffmann & Sgro 2011; La Sorte & Jetz 2012).

The **no-lag hypothesis** proposes that at a given time the species composition of a community is in equilibrium with the observed climate at that location, assuming that an equilibrium can be defined over the temporal or spatial scale of interest (Svenning *et al.* 2015). That is, the species found in a community will have climate niches that are close to the observed climate. The implication is that, in a new climate, species with well-matched niches that are already present will persist, other species with well-matched niches will rapidly immigrate and become present, and species with poorly matched niches will rapidly die and become absent. This hypothesis is implicit in many decades of work assuming that vegetation-climate associations represent consistent physiological responses to environment (von Humboldt & Bonpland 1807 (tr. 2009); Whittaker 1967) and that have often been used to reconstruct climate from paleoecological evidence for pollen, chironomids, diatoms, etc. based on transfer functions (Guiot *et al.* 1989; Gasse *et al.* 1995; Brooks & Birks 2000), coexistence intervals (Mosbrugger & Utescher 1997; Pross *et al.* 2000) or probability densities (Kühl *et al.* 2002). Many of these climate reconstruction approaches assume that species-environment relationships are constant and instantaneous, without considering the consequences of this assumption. The no-lag hypothesis is also implicit in the vast majority of environmental niche modeling / species distribution modeling studies that predict climate change responses (Birks *et al.* 2010; Peterson 2011). This hypothesis is a simple baseline assumption that finds support at multiple scales (e.g., both continental extents over sub-millennial to millennial time scales (e.g. in multi-taxon responses to Younger Dryas climate changes in Switzerland (Birks & Ammann 2000) or across the late Quaternary in North America (Shuman *et al.* 2009; Williams *et al.* 2011)), and is

1
2
3 115 consistent with many species having niches that are well-predicted by their range limits (Lee-
4
5
6 116 Yaw *et al.* 2016). However the hypothesis has also been criticized. One major issue is that its
7
8 117 assumption of very fast species response can be unrealistic (Campbell & McAndrews 1993;
9
10 118 Guisan & Thuiller 2005; Araújo & Peterson 2012). Another important issue is that realized
11
12 119 niches may shift relative to the observed climate due to changes in the available climate space or
13
14 120 in biotic interactions (La Sorte & Jetz 2012; Veloz *et al.* 2012; Maiorano *et al.* 2013). As such,
15
16 121 the realized niche of a species may be a poor proxy for the fundamental niche and may not
17
18 122 necessarily be matched to the observed climate (Jackson & Overpeck 2000; Jordan 2011).
19
20
21 123 Alternatively, **lag hypotheses** argue that the species composition of a community at a
22
23 124 given time is in disequilibrium with contemporary climate (Svenning & Sandel 2013; Blonder *et*
24
25 125 *al.* 2015). That is, the species found in a community may be poorly suited to the climates at the
26
27 126 site, despite other species not occurring in the community having better-suited climate niches
28
29 127 (Davis 1984; Webb 1986; Dullinger *et al.* 2012). Proposed mechanisms include resident species
30
31 128 persisting via survival of long-lived individuals (Eriksson 1996; Holt 2009; Jackson & Sax
32
33 129 2010), species interactions producing micro-scale conditions that remain favorable (Schöb *et al.*
34
35 130 2012; De Frenne *et al.* 2013), or no immigration of more appropriate species because of priority
36
37 131 effects (Fukami *et al.* 2005; Fukami *et al.* 2010), dispersal limitation (Svenning & Skov 2007) or
38
39 132 species absence from the regional pool (Blonder *et al.* 2015). These processes together would
40
41 133 produce a lag between communities' composition and climate. This hypothesis is reflected in a
42
43 134 broad literature showing vegetation lag to climate in forests in the Americas (Webb 1986;
44
45 135 Campbell & McAndrews 1993; Blonder *et al.* 2015) and in Europe (Birks & Birks 2008;
46
47 136 Bertrand *et al.* 2011; Normand *et al.* 2011; Seddon *et al.* 2015), in bird communities (DeVictor *et*
48
49
50
51
52
53
54
55
56
57
58
59
60

1
2
3 137 *al.* 2008), as well as in a range of other paleoecological data (reviewed in Davis (1981) and
4
5 138 Svenning *et al.* (2015)).

6
7
8 139 Here we argue that there is not a dichotomy between lag and no-lag hypotheses. Rather
9
10 140 there is a continuum of lag hypotheses that encompasses more scenarios than have been
11
12 141 previously considered. We show that a broader set of possibilities can lead to unintuitive or
13
14 142 difficult-to-predict community responses. We then provide a set of quantitative tools for
15
16 143 detecting these scenarios in empirical data. Lastly, we demonstrate that simple models of
17
18 144 community processes can generate all of these scenarios.
19
20
21

22 145 23 24 146 **Community response diagrams as diagnostics of dynamics**

25
26
27 147 Lags and lag hypotheses can be measured by comparing a community's composition to the
28
29 148 climate conditions in the community. Making these concepts precise requires defining several
30
31 149 concepts (**Box 1**). These concepts are presented and defined for a single climate axis and variable
32
33 150 (e.g. temperature). They can be extended to multiple climate axes using vector approaches
34
35 151 (Blonder *et al.* 2015), but are illustrated here in a single dimension for clarity.
36
37
38

39 152 First, the location of the community has an **observed climate**, which is given by a
40
41 153 function $F(t)$ (**Fig. 1A**). This variable changes potentially independently from the state of the
42
43 154 community and can be measured without knowledge of the community state, e.g. with a
44
45 155 thermometer for a temperature axis.
46
47

48 156 Second, the community itself has an **inferred climate**, which is given by a function $C(t)$
49
50 157 (**Fig. 1A**). This variable reflects the value of the climate along this axis most consistent with the
51
52 158 occurrence of all species at time t . It can be calculated by overlapping the fundamental niches of
53
54 159 species in the community. For example, a community with cocoa and banana trees would have a
55
56
57
58
59
60

1
2
3
4
5
6
7
8
9
10
11
12
13
14
15
16
17
18
19
20
21
22
23
24
25
26
27
28
29
30
31
32
33
34
35
36
37
38
39
40
41
42
43
44
45
46
47
48
49
50
51
52
53
54
55
56
57
58
59
60

warm inferred climate along a temperature axis, while a community with blueberry and snowberry bushes would have a cold inferred climate. Multiple species assemblages might all yield the same value of $C(t)$.

This concept of $C(t)$ is already widely and implicitly used across fields, although using different terminology. It is widely used in multi-taxon paleoclimate reconstructions (ter Braak & Prentice 1988; Guiot *et al.* 1989; Birks *et al.* 2010; Harbert & Nixon 2015). Additionally, it underlies the definitions in community ecology for a community temperature index (DeVactor *et al.* 2008; Lenoir *et al.* 2013), a floristic temperature (De Frenne *et al.* 2013), and a coexistence interval (Mosbrugger & Utescher 1997; Harbert & Nixon 2015).

Third, the **community climate lag** can be defined as the difference between the observed and the inferred climate (**Fig. 1A**). This metric has been previously used in several studies of ecological disequilibrium (Davis 1984; Webb 1986; Bertrand *et al.* 2011; Blonder *et al.* 2015). If these two values are closely matched, then the lag is small; alternatively, if they are not closely matched, then the lag is large.

These statistics can be visualized and combined with a **community response diagram**. This diagram is a time-implicit parametric plot of the observed climate $F(t)$ on the x-axis and the inferred climate response $C(t)$ on the y-axis (**Fig. 1B**). Using dynamical systems terminology (Katok & Hasselblatt 1997; Beisner *et al.* 2003), $F(t)$ would be considered a parameter (exogenous to the system) and $C(t)$ would be considered a state variable (endogenous to the system). The diagram is similar to a phase space diagram of dynamical systems research (e.g. Sugihara *et al.* (2012)) that plots multiple state variables as time-implicit curves, but is different in that $F(t)$ is not a state variable. It also is similar to the ball-in-cup landscapes used in ecosystem resilience / regime shift / alternate stable states research (e.g. Beisner *et al.* (2003);

Scheffer and Carpenter (2003)) that also combine a parameter with a state variable. However this diagram differs in that it shows the actual trajectory of the state variable over time, rather than the cost of taking different trajectories at a single point in time. That is, a community response diagram integrates the trajectories on a continually deforming ball-in-cup landscape, and does not directly describe the stability or temporal dynamics of the community at any time point. As such, it is useful for addressing different questions than these other graphs, in particular questions of unstable or disequilibrium community responses to changing climate.

By plotting the community's response as a function of the climate forcing, the continuum of lag hypotheses can be described and distinguished with two novel statistics. The first statistic is the **mean absolute deviation**, $|\overline{\Delta}|$, which describes the average absolute difference between $C(t)$ and $F(t)$ over time (**Fig. 2A**). A value statistically indistinguishable from zero indicates no lag and larger values indicates a lag (positive or negative). The second statistic is the **maximum state number**, n , which counts the maximum number of values of $C(t)$ that correspond to a single value of $F(t)$ (**Fig. 2B**). Considering the community response diagram as a curve in the F - C plane, n is the maximum number of intersection points of any vertical line. If there is only one value of $C(t)$ corresponding to each value of $F(t)$, then $n=1$, and the community has dynamics that can always be predicted from knowledge of the current value of $F(t)$. If n becomes larger, then the community can have possible multiple states for a single observed climate. In these cases it becomes increasingly less possible to predict the community's state with knowledge of only the observed climate. Thus, the maximum state number provides a simple way to assess the limits to predictability for community dynamics.

A continuum of lag scenarios on a community response diagram

There are several general scenarios for the coupling between climate change and community response that yield different $C(t)$ vs. $F(t)$ trajectories on a community response diagram (**Fig. 3**). Each of these scenarios also yields a different combination of values for the $|\overline{\Lambda}|$ and n statistics. Therefore values of these statistics can be used to delineate hypotheses along the lag continuum.

The first scenario corresponds exactly to the **no-lag** hypothesis: in this case $\Lambda(t) = 0$, so $C(t) = F(t)$. This is equivalent to a straight-line segment with slope of 1 and intercept of 0 on the community response diagram for any possible observed climate $F(t)$ (**Fig. 3A**). In this scenario $n=1$ and $|\overline{\Lambda}|=0$. Here, equality is statistically defined relative to natural variation, e.g. $\sigma(t)$.

The second scenario corresponds to a **constant-relationship** lag hypothesis. In this case, $|\Lambda(t) \geq 0|$ and $C(t) = f(F(t))$. Because f is a function, then there is always a single unique value of $C(t)$ corresponding to a unique value of $F(t)$. However the opposite is not true: there may be multiple values of $F(t)$ that all correspond to the same value of $C(t)$. That is, the community's inferred climate is uniquely determined by the observed climate at any given time. This is equivalent to a single curve on the community response diagram that never crosses itself for any observed climate, so $n=1$ and $|\overline{\Lambda}| > 0$ (**Fig. 3B**).

The third scenario corresponds to the **constant-lag** hypothesis. In this case, $|\Lambda(t)| > 0$ and $C(t) = \alpha F(t - \phi)$ for some value α . If $F(t)$ is a periodic function, then this corresponds to a fold on the community response diagram, i.e. a scenario where $F(t)$ crosses over itself (**Fig. 3B**). In the case of a sinusoidal $F(t)$, the shape will be a single loop, with the elongation of the loop being related to the amount of lag (**Fig. 3C**). Such a scenario always has a value of $n=2$ and $|\overline{\Lambda}| > 0$.

However, for a linear $F(t)$ function, the shape will be a straight line with slope not necessarily equal to 1 and intercept not necessarily equal to 0. That scenario reduces to the constant-relationship conceptualization and has $n=1$ and $|\overline{\Lambda}|>0$. In general the presence of a fold or loop in the community response diagram indicates **memory effects (hysteresis)**, such that the future state of the system depends on its past history (Katok & Hasselblatt 1997) (**Fig. 3D**). Systems with memory effects have path dependence. That is, the future dynamics of the community cannot be predicted only by knowing the current community state, but rather by also using the past state of the community. Larger values of $|\overline{\Lambda}|$ correspond to more memory effects.

The fourth scenario, **alternate unstable states**, is a generalized version of the third scenario, describing a community response diagram that contains multiple folds (**Fig. 3E**). At any given value of $F(t)$, the future state of the community depends on its past state. If $F(t)$ is periodic, then the community response diagram will contain multiple loops corresponding to stable orbits. At any of the intersections between loops, determining which path the community takes will depend on knowledge of its past state. Alternatively if the system has a stable orbit but has not yet reached it because of **transient effects**; then there may be large lags between $C(t)$ and $F(t)$ while the system settles to a steady state (**Fig. 3C**). These scenarios are all reflected in a value of $2 \leq n < \infty$ and $|\overline{\Lambda}|>0$. Critically, these alternate states are not necessarily equivalent to the alternate stable states that have been previously studied (Beisner *et al.* 2003). They may not persist in time, and the community state is not necessarily attracted to them, although both scenarios are admissible. The key point here is that single values of the observed climate can lead to multiple values of the community state.

The fifth scenario, **unpredictable dynamics**, corresponds to a scenario where there are no stable orbits and a very large number of possible relationships between the observed climate

1
2
3 250 and the composition of the community. Predicting the future state of the community is very
4
5 251 difficult, because arbitrarily large changes in the community's future state can occur regardless
6
7
8 252 of changes in values of the past community state or observed climate. In this case $n_{\max} \rightarrow \infty$ and
9
10
11 253 $|\overline{\Lambda}| > 0$. These dynamics can occur via **chaos** (Lorenz 1995), when the future community state is
12
13
14 254 deterministic but very sensitive to variation in the present and past community state, where any
15
16 255 state of the system is eventually reached from any other past state of the system, and where
17
18 256 dynamical orbits are dense (**Fig. 3F**). Unpredictable dynamics can also occur when the future
19
20
21 257 state of the community is not a deterministic response to any variable, as in the previous five
22
23 258 scenarios, but rather is a **stochastic response**. In this case, $C(t)$ and $F(t)$ can become partially or
24
25
26 259 completely uncorrelated, and a range of points in the community response diagram can become
27
28 260 filled in (**Fig. 3G**). For example, random immigration and emigration of species from a regional
29
30 261 species pool can yield fluctuations in $C(t)$ (Holyoak *et al.* 2005)), while the climate system drives
31
32
33 262 fluctuations in $F(t)$. Alternatively, $C(t)$ may be determined primarily by internal processes (e.g.
34
35 263 species interactions, anthropogenic factors) rather than external climate-mediated processes,
36
37 264 leading to a complete decoupling of $C(t)$ and $F(t)$. For example, many North American and
38
39
40 265 European forests are thought to have been managed for food production throughout the Holocene
41
42 266 (Mason 2000; Abrams & Nowacki 2008), and many invasive species have colonized new regions
43
44
45 267 due to enemy release (Keane & Crawley 2002), leading to geographic range shifts that are
46
47 268 unrelated to climate change.

48
49 269 Each of these scenarios has different consequences for predictability in community
50
51 270 ecology. The first two scenarios (no lag, constant-relationship lag) represent scenarios where
52
53 271 prediction of future community states is readily possible. These scenarios have received the
54
55
56 272 majority of study in community ecology, perhaps rightly. Nevertheless, the latter three scenarios
57
58
59
60

are also conceptual possibilities. They challenge the assumptions of many research paradigms, because they imply there is no longer a simple or one-to-one relationship between climate conditions and community state. If constant-lag, alternative unstable states, or unpredictable dynamics were to occur, then modeling a community's future state would be a challenge. With knowledge of only future observed climate, the task might be impossible; even with knowledge of the past observed climate and community state, the task might be very difficult. The consequence would be limited predictability in community ecology and shortened ecological forecast horizons (Petchey *et al.* 2015).

A simple analytic model for lags in community dynamics

All of the scenarios along the lag continuum can arise within a simple differential equation model for community dynamics (**Box 2**). The model abstracts and summarizes the community-scale effect of two species-scale processes: a **tracking** effect, in which communities try to restore themselves toward an optimal climate state, and a **resistance** effect, in which communities try to maintain their current (or past) composition. Temporal variation in the observed climate acts as a forcing for the model, while the interplay between the tracking and resistance processes determines the directionality and strength of the community's response. The resistance and tracking effects are intended as proxies for a range of real ecological processes occurring for individual species. By abstracting these lower scale processes we hope to gain general insights about possible dynamics at community-scale. Both resistance and tracking must emerge from dispersal limitation, species interactions, environmental filtering, or adaptation (Wisz *et al.* 2013; Singer *et al.* 2016; Zurell *et al.* 2016). For example, if some species in a regional pool have a limited ability to disperse into a community, then tracking will be

1
2
3 296 weaker. Similarly, resistance could be stronger if residents have advantages over invaders that
4
5
6 297 must disperse in. If species interactions lead to established species persisting more easily than
7
8 298 invader species can establish, then resistance will be stronger. Stronger environmental filtering
9
10 299 could lead to stronger tracking by removing species with niches that yield low performance.
11
12 300 Adaptation could yield both stronger tracking by shifting species' niches or stronger resistance
13
14
15 301 by enabling species to maintain their niches. Our intent here is not to develop specific models
16
17 302 that link these species-scale processes to community-scale effects, but rather to highlight how
18
19 303 different types of such models would lead to different community outcomes. This exercise
20
21
22 304 reveals several general principles of community dynamics. These conclusions are all
23
24 305 mathematically true regardless of how the species-scale processes come together to yield a given
25
26 306 set of restorative and tracking effects. First, linear climate change can only lead to no-lag,
27
28 307 constant delay, or constant-relationship scenarios regardless of all other model parameters,
29
30 308 including the time delay Δt . However, under periodic climate change, all lag scenarios are
31
32 309 possible. When the tracking and resistance effects are restorative, the system is characterized by
33
34 310 transient dynamics towards a stable orbit. During the transient stage, n can become arbitrarily
35
36 311 large, strongly limiting the ability to predict future states. The stronger the relative effect of the
37
38 312 restorative effect, the longer the transient behavior persists. However, $C(t)$ will eventually settle
39
40 313 to a stable orbit with the same frequency as the observed climate $F(t)$. Depending on the exact
41
42 314 form of the model, this steady orbit may constitute constant delay dynamics, but may also exhibit
43
44 315 alternate unstable states with multiple loops. If the restorative effect pulls the system toward a
45
46 316 fixed state with time-delay (e.g. strong selection for a certain forest type regardless of climate),
47
48 317 then along with the scenarios above, for different parameter regimes the system can also exhibit
49
50
51
52
53 318 transient dynamics converging to alternate states with high n , as well as chaos.
54
55
56
57
58
59
60

The example community trajectories diagrammed in **Figure 3** for each conceptual scenario correspond to dynamics predicted by this model for different parameter combinations. Specific parameter values are given in **Table S1**. However the numeric values are less important than the general conclusion that the combination of restorative forces with time delay and climate tracking can lead to complex and widely varied dynamics, even in a simplified model. There are three conceptual implications arising from this modeling exercise that will be relevant to all observational and theoretical studies of community dynamics.

First, the observation of a lag between the observed climate and the community response does not immediately indicate anything about the rules governing the system. Most scenarios show memory effects, so that knowledge of the past state of climate and community are needed to predict the system's future state. This result challenges the reliability of correlative methods for inferring the role of environmental drivers in community responses, because of the strong role of history on contemporary patterns (Dupouey *et al.* 2002; Willis *et al.* 2013). Nevertheless, for individual species, the success of species distribution models in predicting across space and time (Svenning & Sandel 2013) and the partial congruence of range limits and niche limits (Hargreaves *et al.* 2014; Lee-Yaw *et al.* 2016) suggest that simple no-lag approaches are viable. The major challenge will come in integrating species-scale predictions to community-scale responses where species-stacking approaches may fail because of interactions between species.

Second, small changes in a model's definitions can lead to qualitatively different types of ecological dynamics. This indicates that complex dynamics may become relevant in natural communities. Indeed, lagged dynamics with memory effects and state numbers of $n \geq 2$ are easy to generate in the particular model we presented here.

1
2
3
4
5
6
7
8
9
10
11
12
13
14
15
16
17
18
19
20
21
22
23
24
25
26
27
28
29
30
31
32
33
34
35
36
37
38
39
40
41
42
43
44
45
46
47
48
49
50
51
52
53
54
55
56
57
58
59
60

341 Third, the frequency of climate change relative to the community response capacity is
342 important in determining the type of dynamics that arise (Sastry 2013). When the observed
343 climate varies at much lower frequencies than the capacity of the community to respond, then the
344 climate change is linear or effectively linear over the time period of interest, so no-lag or
345 constant relationship dynamics are likely to dominate (Williams *et al.* 2011). Similarly, when the
346 observed climate varies at much higher frequencies than the capacity of the community to
347 respond, then unpredictable dynamics are likely to dominate unless the climate varies rapidly
348 about a constant mean; then the community may show limited response, as for example the case
349 of *Populus tremuloides* – dominated communities that persist across glacial-interglacial
350 transitions (Mitton & Grant 1996). Finally, when the observed climate varies at frequencies
351 comparable to the community’s response capability, then alternate unstable state or unpredictable
352 dynamics may become important.

354 **Practical conceptual considerations**

355 A natural question arising from these conceptual and analytical arguments is: which scenarios
356 are likely to be found in the natural world? That is, is predictability achievable in practice, or
357 not? The framework we have proposed could be applied to empirical data to answer this
358 question. The scope of this article prevents presentation of such an analysis, so we instead focus
359 on highlighting several issues that should be considered before implementing the framework.

360 Describing patterns of lags and testing lag hypotheses can be achieved by estimating $C(t)$
361 and $F(t)$ from data. If both time-series are obtained from a finite number of empirical samples
362 $\{C(t_i), F(t_i)\}$, then the easiest way to calculate both statistics is through approximation. Values
363 of $\overline{|\Lambda|}$ can be obtained by averaging sampled values of $|C(t_i) - F(t_i)|$. Values of n can be

calculated by linearly interpolation between successive values of $C(t_i)$ and $F(t_i)$ followed by application of line intersection methods. Measurement uncertainty or other noise arising in both $C(t)$ and $F(t)$ can be problematic when counting the maximum state number or determining whether a community response diagram contains loops. For example, suppose the community at two time points t_1 and t_2 has $F(t_1)=F(t_2)$, but $|C(t_1) - C(t_2)| < \max(\sigma(t_1), \sigma(t_2))$. In this case, the community takes two different states for a given observed climate, suggesting $n \geq 2$, but those states may not be sufficiently different to be confident that the difference is statistically significant. Regardless, the general qualitative implication is that estimation uncertainty and noise in time series can overestimate the maximum state number. Alternatively, low sampling resolution or a low number of points in a time series can lead to underestimation of n . Small loops or folds can be missed if they appear and disappear more rapidly than the sampling permits. We therefore recommend that community trajectories should be potentially rounded to the nearest multiple of $\sigma(t)$ and also smoothed before analysis (e.g. with cubic splines) (**Fig. 2**). We have implemented methods to calculate n and $|\overline{\Lambda}|$, taking into account statistical uncertainty in data, as R functions in **Supplementary Data S2**.

Determining the underlying processes that have generated an empirical community response diagram is possible by fitting an analytic model to observed data for $C(t)$ and $F(t)$. There are several methods available to reconstruct a differential equation for $C(t)$ based on observations of $C(t)$ and $F(t)$ at different times. For example, generalized additive models with terms describing different effects can be fitted to numerical estimates of the first derivative of $C(t)$, providing a direct reconstruction of a differential equation (Ellner *et al.* 1997). It is also possible to estimate equation parameters from knowledge of the distribution of time intervals between extremes in a dataset (Bezruchko *et al.* 2001). Alternatively, equation-free approaches

1
2
3
4
5
6
7
8
9
10
11
12
13
14
15
16
17
18
19
20
21
22
23
24
25
26
27
28
29
30
31
32
33
34
35
36
37
38
39
40
41
42
43
44
45
46
47
48
49
50
51
52
53
54
55
56
57
58
59
60

for predicting the future state of a system based on its past state may also be viable (Sugihara *et al.* 2012; Ye *et al.* 2015). However all of these approaches tend to require data sampled at hundreds of different times, which may not be achievable for ecological data.

In either application, it may be difficult to distinguish among transient, chaotic, and stochastic dynamics. For finite numbers of samples, these all lead to coarsely similar community response diagrams. When sampling of $C(t)$ and $F(t)$ is infrequent or includes measurement errors, it may be difficult to separate signal from noise in community response diagrams. Formal tests for distinguishing chaos from noise based on embedding of dynamical systems do exist (Gottwald & Melbourne 2004). Only with very long time series and precise measurements would it be possible to distinguish these scenarios in practice.

Lastly, it may be challenging to make unbiased measurements of $C(t)$. Because $C(t)$ depends on knowing the modal niche value for each species, any bias in species' estimating species niches may also propagate to community-scale statistics. Realized niche estimates based on contemporary geographic occurrences of species may be particularly biased and themselves show lags (Jackson & Overpeck 2000; Soberón & Nakamura 2009), but provide the simplest method for calculating these statistics ((Blonder *et al.* 2015).

Practical data considerations

Finding data to infer community response diagrams remains a challenge. A representative sample of the community's composition is required to estimate $C(t)$. Time series of community dynamics are rare because of the long timescales and high efforts involved in this sampling. The best example is probably from the Park Grass Experiment in England, comprising dozens of censuses between 1856 and 2006 (Silvertown *et al.* 2006). On the other hand, the 50-ha forest

dynamics plot at Barro Colorado Island (Panama) has been censused only seven times between 1980 and 2010 (Condit *et al.* 2012), and the macrophyte communities at Loch Leven (Scotland) have been censused only eight times between 1905 and 2008 (Dudley *et al.* 2012). Temporal extent is less important than number of time points: for example, it is possible to compare vegetation change on Chimborazo volcano (Ecuador) between 1802 and 2012, but measurements are only available at those two time points (Morueta-Holme *et al.* 2015). Other highly-sampled time series, e.g. the Isle Royale (United States) wolf-moose dataset (Vucetich & Peterson 2012), are oriented towards a single focal species rather than whole communities.

However there are some systems where representative samples of communities at multiple time points are available. Microcosm studies of provide one possibility, e.g. protist communities (Petchey *et al.* 1999); similarly, metagenomics approaches are making community dynamics in microbial communities increasingly accessible (Faust *et al.* 2015). Alternatively, at longer time scales, paleoecological assemblage datasets may provide proxies for community dynamics. For example, fossil pollen assemblages for eastern North America are available for the last 21 Kyr at 500 yr resolution, e.g. Maguire *et al.* (2016). Indeed, many of the studies that have calculated inferred climate time series using other approaches, e.g. Mosbrugger and Utescher (1997); Köhl *et al.* (2002); DeVicor *et al.* (2008); Bertrand *et al.* (2011), could be recast in terms of $C(t)$. In these cases the challenge would be to make estimates of $F(t)$ for these communities that are independent of the community data. In the case of late Quaternary climate change, paleoclimate simulations based on general circulation models provide proxies for $F(t)$, but spatial and temporal resolution still remains coarse (Lorenz *et al.* 2016). For more contemporary time series, meteorological data may instead be available, e.g. Bertrand *et al.* (2011). Better understanding the limitations and potential of these various datasets, as well as

1
2
3
4
5
6
7
8
9
10
11
12
13
14
15
16
17
18
19
20
21
22
23
24
25
26
27
28
29
30
31
32
33
34
35
36
37
38
39
40
41
42
43
44
45
46
47
48
49
50
51
52
53
54
55
56
57
58
59
60

actively collecting more time-series community data, remains an ongoing but important monitoring challenge for ecology.

Implications and synthesis

We showed that community response diagrams comprising plots of $F(t)$ and $C(t)$ provide methods to assess and understand how climate drives disequilibrium community states. By measuring lags with these community trajectories, and by calculating mean absolute deviations and maximum state numbers, we are able to provide approaches to assess the continuum of lag hypotheses, determine the limits to predictability, and assess the importance of a community's past on its future.

The possibility of memory effects underscores the challenges present in predictive community ecology. Hysteresis is known to limit the ability of systems to return to an original stable state (Beisner *et al.* 2003; Folke *et al.* 2004), but our work now shows that unstable communities are also not guaranteed to return to the same state when the observed climate takes a previous value. This may provide a complementary explanation for why returning environments to historical conditions is unlikely to result in community shifts toward historical states: regime shifts can occur when the history of the community determines which future compositional state will be obtained (Scheffer & Carpenter 2003). Additionally, hysteresis suggests that commonly used space-for-time substitutions may not be appropriate, because the temporal dynamics of a system will depend on the past community state, while the spatial dynamics will not. Lastly, it also suggests that conservation efforts that take actions to reduce climate lags (such as assisted migration, rewilding, or restoration of historical states) may potentially yield unexpected outcomes.

The niche axes comprising $C(t)$ and $F(t)$ can include any variables that mediate species response to environment. Here we defined them in terms of climate variables. However, edaphic variables could also be important, given the close association between species occurrence and soil conditions. Soil legacies can persist for 10^3 - 10^4 years (Dupouey *et al.* 2002) and many species' distributions are very sensitive to soil conditions (Harrison 1999; Silvertown *et al.* 1999; Asner & Martin 2016), with community lags being driven by soil development (Kuneš *et al.* 2011).

The community response diagrams could also be recast in terms of functional traits, where $F(t)$ is an optimum trait value, and $C(t)$ is a community-weighted mean trait value (Garnier *et al.* 2004). Shifts and lags in trait-environment relationships (Kimberley *et al.* 2016; van der Sande *et al.* 2016) or skewness in trait distributions (Enquist *et al.* 2015) may be explainable using this approach. Remotely-sensed community-weighted mean traits and remotely-sensed climate data may be appropriate to explore this idea (e.g. Seddon *et al.* (2016)).

A next step toward more mechanistic understanding of community dynamics will be to couple the community-scale differential equation models to process-based models for individuals and populations of species in regional pools. By assessing the individual and combined effects of different types and strengths of dispersal limitation, species interactions, and environmental filtering on community-scale patterns, it could become possible to identify the most likely drivers of each type of dynamics. Understanding the processes that lead to predictability and those that do not would help delineate when community ecology can hope to become more predictive (Fukami 2015), and when forecast horizons must remain small (Petchey *et al.* 2015).

Conclusion

1
2
3 479 We have explored some of the limits to predictability in community ecology by using
4
5
6 480 community response diagrams. The overall implication of this work is that predicting community
7
8 481 response to past and near-future climate change will be difficult because of the diversity of
9
10 482 possible dynamics. The no-lag hypothesis implicit in contemporary species distribution modeling
11
12 483 represents a very narrow class of dynamics that may be successful at the scale of single species
13
14
15 484 but not successful at the emergent community scale. The constant-lag and constant relationship
16
17 485 lag hypotheses of contemporary disequilibrium ecology and the extensions of species
18
19
20 486 distribution modeling that incorporate dispersal limitation also represent a limited class of
21
22 487 dynamics. There is evidence that some communities have sensitive responses to climate change
23
24 488 (Ackerly 2003; Shuman *et al.* 2009; Nogué *et al.* 2013) and can exhibit regime shifts (Folke *et*
25
26 489 *al.* 2004), whereas some others do not show evidence for this (Nowacki & Abrams 2015).
27
28
29 490 Similarly, evidence for niche equilibrium at species scale is highly mixed (Veloz *et al.* 2012;
30
31 491 Lee-Yaw *et al.* 2016). The possible existence of alternate unstable states and unpredictable
32
33 492 dynamics should lead to careful consideration of whether extant approaches have oversimplified
34
35 493 our perception of community dynamics.
36
37
38 494 Better delineating when and why responses to climate change will differ among
39
40 495 communities should become a priority. Progress on predicting rather than explaining dynamics
41
42 496 remains elusive and will require better understanding how processes such as species interactions
43
44 497 and dispersal limitation determine the dynamical rules for community dynamics in response to
45
46 498 climate change. We therefore suggest caution in our ability to make robust predictions about the
47
48
49
50 499 future.
51
52
53
54
55
56
57
58
59
60

Acknowledgments

We also thank the Center for Macroecology, Evolution, and Climate at Copenhagen University, Center for Biodiversity Dynamics at the Norwegian University of Science and Technology, and Jarle Tufto for helpful feedback. Several anonymous reviewers also greatly improved the manuscript. This work was supported by a UK Natural Environment Research Council independent research fellowship (NE/M019160/1) and a Norwegian Research Council Klimaforsk grant (250233). AO and JCS were supported by the European Research Council (ERC-2012-StG-310886-HISTFUNC to JCS).

510

512 described by **Table 1** and shown in **Figure 3**.

517

Supplementary Table S1 - Examples of model parameters that generate each class of dynamics, corresponding to the panels in **Fig. 3**. Many other parameter combinations can also generate each of these scenarios; this list is not meant to be exhaustive. Fields marked as '-' can take any value without changing the dynamics.

Scenario	Panel	C _T	C _R	Δt	R(ρ)	T(τ)	ρ	τ	C ₀	F(t)	
No lag	a	0	∞	any	-	τ	-	C(t) – F(t)	-	sin(t)	
Constant delay	b	0.2	10	5	sin(ρ) • exp(-p ²)	τ	C(t) – C(t-Δt)	C(t) – F(t)	-	t	
Constant relationship	b	same as above as t->∞									
Transient dynamics	c	1	5	5	ρ	τ	C(t) – C(t-Δt)	C(t) – F(t)	-	sin(t)	
Constant delay	c	same as above as t->∞									
Memory effects	d	1	15	3.5	ρ ³	τ	C(t) – C(t-Δt)	C(t) – F(t)	-	sin(t)	
Alternate states	e	1	8	15	sin(ρ) • exp(-p ²)	τ	C(t-Δt)-C ₀	C(t) – F(t)	0.2	sin(t)	
Chaos	f	1	8	16	sin(ρ) • exp(-p ²)	τ	C(t-Δt)-C ₀	C(t) – F(t)	0.35	sin(t)	
Stochastic	g	not applicable – C(t) simulated as smoothed Brownian motion									sin(t)

522

523

For Review Only

1
2
3
4
5
6
7
8
9
10
11
12
13
14
15
16
17
18
19
20
21
22
23
24
25
26
27
28
29
30
31
32
33
34
35
36
37
38
39
40
41
42
43
44
45
46
47
48
49
50
51
52
53
54
55
56
57
58
59
60

Supplementary Text S1. An upper bound on the maximum state number n .

The bound comes as a consequence of the observation that if both F and C are periodic, then the response diagram in the F - C plane will form a closed curve. It is evident that any vertical line can only intersect a closed curve a finite number of times; hence the state number is finite. Further, for a closed curve, the maximum number of intersection points of a vertical line cannot be larger than the number of vertical fold points, i.e. points where $\frac{dF}{dt} = 0$. This follows from the fact that on either side of an intersection point, the curve must fold back in order to form a closed curve. If we define P_F to be the period of $F(t)$, and P_C the period of $C(t)$, then the period P of the system (time for F and C to both return to the same value) will satisfy $P = aP_C = bP_F$, where a and b are mutually prime integers. Then, if $\frac{dF}{dt} = 0$ k times in one period P_F , then we have the bound

(S1-1)
$$n \leq kb$$

For example, considering simple sinusoids $F(t) = \sin(t)$, $C(t) = \sin(\frac{t}{m})$, with $m \geq 1$ an integer (because F forces C and not the other way around, C will typically have longer [or equal] period than F). This gives $k = 2$ and $b = m$, the least common multiple of their periods. A larger value of b implies that the observed climate must cycle more times before the community response repeats, and thus one value of F can correspond to more values of C . A larger value of k , on the other hand, implies a more complex observed climate.

While this result is only strictly valid for continuous periodic functions $C(t)$ and $F(t)$, the basic idea can be extended to empirical time series of $C(t)$ and $F(t)$ that are approximately periodic. For instance, if the Fourier spectra of $C(t)$ and $F(t)$ are dominated by particular wavelengths, then approximations for a and b may be computed and the arguments above may be applied.

Supplementary Text S2. Transient behavior of the model described in **Box 2**.

To understand the nature of transient effects and the parametric dependence, we analyze the case of linear tracking and linear resistance, $T(x) = R(x) = x$, for which analytical progress can be made. We use **Equation B2-3** for ρ . In this case, **Equation B2-1** can be expressed as

$$(S2-1) \quad \frac{dC(t)}{dt} + c_T C(t) + c_R (C(t) - C(t - \Delta t)) = c_T F(t)$$

The solution is the sum of a solution of the homogeneous equation, with zero right hand side, and a particular solution. Seeking a solution of the homogeneous equation in the form $C(t) = Ae^{\lambda t}$ leads to the transcendental equation $\lambda + c_T + c_R - c_R e^{-\Delta t \lambda} = 0$. We seek solutions in the complex plane: taking $\lambda = x + iy$ and separating real and imaginary parts gives the set of equations

$$(S2-2) \quad \begin{aligned} x + c_T + c_R &= c_R e^{-\Delta t x} \cos(\Delta t y) \\ y &= c_R e^{-\Delta t x} \sin(\Delta t y) \end{aligned}$$

We begin by showing that any solution will be characterized by $x < 0$. First, note that when $\Delta t = 0$, the only solution is $y = 0$, and $x = -c_T < 0$. In order to have $x > 0$, it must cross the axis, i.e. there must be a value of Δt for which $x = 0$. However, setting $x = 0$ gives $\cos(\Delta t y) = \frac{c_T + c_R}{c_R} > 1$, for which there can be no solutions. Therefore, the homogeneous solution is always characterized by exponential decay.

Once the homogeneous solution sufficiently decays, $C(t)$ follows the particular solution, whose form will be driven by the form of $F(t)$. For example, in the case of sinusoidal forcing (**Equation B2-10**), the particular solution may be constructed explicitly as a combination of $\sin(\omega t)$ and $\cos(\omega t)$. This shows (for the linear case) that after transients decay, the system settles into a periodic state with equivalent frequency to the forcing. While the situation is less

1
2
3
4
5
6
7
8
9
10
11
12
13
14
15
16
17
18
19
20
21
22
23
24
25
26
27
28
29
30
31
32
33
34
35
36
37
38
39
40
41
42
43
44
45
46
47
48
49
50
51
52
53
54
55
56
57
58
59
60

straightforward with nonlinear tracking and resistance functions, the general structure of transient decay towards a solution with the same form as $F(t)$ has generally been observed in all of our numerical simulations.

The duration of the transient effects is determined by the value of x closest to 0. Considering the graphs of the curves $f(x) = \frac{x}{c_R} + 1 + \frac{c_T}{c_R}$, $g(x) = e^{-\Delta t x} \cos(\Delta t y)$, whose intersections define the rate of decay of transients, we see that in the limit $\frac{c_T}{c_R} \rightarrow 0$, $f(x)$ approaches a vertical line with intercept at $f(0) = 1$, and thus intersection points x^* for which $f(x^*) = g(x^*)$ approach 0 from the left. In the other limit, $\frac{c_T}{c_R} \rightarrow \infty$, there is only a single root $x^* \rightarrow -c_T$. The transient time increases with decreasing ratio $\frac{c_T}{c_R}$, i.e. as resistance effects dominate tracking effects.

This simple analysis also suggests a strong difference in the potential behavior exhibited with lagged resistance to a constant state, that is when ρ is given by **Equation B2-4**. Here **Equation S2-2** becomes

(S2-3)
$$\begin{aligned} x + c_T &= -c_R e^{-\Delta t x} \cos(\Delta t y) \\ y &= -c_R e^{-\Delta t x} \sin(\Delta t y) \end{aligned}$$

These equations do admit solutions with non-negative x . Thus there are parameter regimes in the linear case where the transient grows with time, even while the community is restoring toward a constant state.

References Cited

1. Abrams, M.D. & Nowacki, G.J. (2008). Native Americans as active and passive promoters of mast and fruit trees in the eastern USA. *The Holocene*, 18, 1123-1137.
2. Ackerly, D. (2003). Community Assembly, Niche Conservatism, and Adaptive Evolution in Changing Environments. *International Journal of Plant Sciences*, 164, S165-S184.
3. Araújo, M.B. & Peterson, A.T. (2012). Uses and misuses of bioclimatic envelope modeling. *Ecology*, 93, 1527-1539.
4. Asner, G.P. & Martin, R.E. (2016). Convergent elevation trends in canopy chemical traits of tropical forests. *Global Change Biology*, 22, 2216-2227.
5. Beisner, B.E., Haydon, D.T. & Cuddington, K. (2003). Alternative stable states in ecology. *Frontiers in Ecology and the Environment*, 1, 376-382.
6. Bertrand, R., Lenoir, J., Piedallu, C., Riofrio-Dillon, G., de Ruffray, P., Vidal, C. *et al.* (2011). Changes in plant community composition lag behind climate warming in lowland forests. *Nature*, 479, 517-520.
7. Bezruchko, B.P., Karavaev, A.S., Ponomarenko, V.I. & Prokhorov, M.D. (2001). Reconstruction of time-delay systems from chaotic time series. *Physical Review E*, 64, 056216.
8. Birks, H. & Birks, H.H. (2008). Biological responses to rapid climate change at the Younger Dryas—Holocene transition at Kråkenes, western Norway. *The Holocene*, 18, 19-30.
9. Birks, H.H. & Ammann, B. (2000). Two terrestrial records of rapid climatic change during the glacial–Holocene transition (14,000–9,000 calendar years BP) from Europe. *Proceedings of the National Academy of Sciences*, 97, 1390-1394.
10. Birks, H.J.B., Heiri, O., Seppä, H. & Bjune, A.E. (2010). Strengths and Weaknesses of Quantitative Climate Reconstructions Based on Late-Quaternary Biological Proxies. *Open Ecology Journal*, 3, 68-110.
11. Blonder, B., Nogués-Bravo, D., Borregaard, M.K., Donoghue Ii, J.C., Jørgensen, P.M., Kraft, N.J.B. *et al.* (2015). Linking environmental filtering and disequilibrium to biogeography with a community climate framework. *Ecology*, 96, 972-985.
12. Boyd, J. (2013). Finding the Zeros of a Univariate Equation: Proxy Rootfinders, Chebyshev Interpolation, and the Companion Matrix. *SIAM Review*, 55, 375-396.
13. Brooks, S.J. & Birks, H. (2000). Chironomid-inferred late-glacial and early-Holocene mean July air temperatures for Kråkenes Lake, western Norway. *Journal of Paleolimnology*, 23, 77-89.
14. Campbell, I.D. & McAndrews, J.H. (1993). Forest disequilibrium caused by rapid Little Ice Age cooling. *Nature*, 366, 336-338.
15. Condit, R., Lao, S., Pérez, R., Dolins, S.B., Foster, R. & Hubbell, S. (2012). Barro Colorado Forest Census Plot Data (Version 2012). Center for Tropical Forest Science Databases.
16. Davis, M.B. (1981). Quaternary History and the Stability of Forest Communities. In: *Forest Succession: Concepts and Application* (eds. West, DC, Shugart, HH & Botkin, DB). Springer New York New York, NY, pp. 132-153.
17. Davis, M.B. (1984). Climatic instability, time, lags, and community disequilibrium. In: *Community Ecology* (eds. Diamond, J & Case, TJ). Harper & Row New York, pp. 269-284.

1
2
3 632 18. De Frenne, P., Rodríguez-Sánchez, F., Coomes, D.A., Baeten, L., Verstraeten, G.,
4 633 Vellend, M. *et al.* (2013). Microclimate moderates plant responses to macroclimate
5 634 warming. *Proceedings of the National Academy of Sciences*, 110, 18561-18565.
6 635 19. DeVicor, V., Julliard, R., Couvet, D. & Jiguet, F. (2008). Birds are tracking climate
7 636 warming, but not fast enough. *Proceedings of the Royal Society of London B: Biological*
8 637 *Sciences*, 275, 2743-2748.
9 638 20. Dorrie, H. & Antin, D. (1965). Sturm's Problem of the Number of Roots. In: *100 Great*
10 639 *Problems of Elementary Mathematics: their history and solution*. Dover Publications
11 640 New York, pp. 112-116.
12 641 21. Dudley, B., Gunn, I.D.M., Carvalho, L., Proctor, I., O'Hare, M.T., Murphy, K.J. *et al.*
13 642 (2012). Changes in aquatic macrophyte communities in Loch Leven: evidence of
14 643 recovery from eutrophication? *Hydrobiologia*, 681, 49-57.
15 644 22. Dullinger, S., Gatttringer, A., Thuiller, W., Moser, D., Zimmermann, N.E., Guisan, A. *et al.*
16 645 (2012). Extinction debt of high-mountain plants under twenty-first-century climate
17 646 change. *Nature Climate Change*, 2, 619-622.
18 647 23. Dupouey, J.L., Dambrine, E., Laffite, J.D. & Moares, C. (2002). Irreversible impact of
19 648 past land use on forest soils and biodiversity. *Ecology*, 83, 2978-2984.
20 649 24. Ellner, S.P., Kendall, B.E., Wood, S.N., McCauley, E. & Briggs, C.J. (1997). Inferring
21 650 mechanism from time-series data: Delay-differential equations. *Physica D: Nonlinear*
22 651 *Phenomena*, 110, 182-194.
23 652 25. Enquist, B.J., Norberg, J., Bonser, S.P., Violle, C., Webb, C.T., Henderson, A. *et al.*
24 653 (2015). Scaling from Traits to Ecosystems: Developing a General Trait Driver Theory via
25 654 Integrating Trait-Based and Metabolic Scaling Theories. *Advances in Ecological*
26 655 *Research*, 52, 249-318.
27 656 26. Eriksson, O. (1996). Regional Dynamics of Plants: A Review of Evidence for Remnant,
28 657 Source-Sink and Metapopulations. *Oikos*, 77, 248-258.
29 658 27. Faust, K., Lahti, L., Gonze, D., de Vos, W.M. & Raes, J. (2015). Metagenomics meets
30 659 time series analysis: unraveling microbial community dynamics. *Current Opinion in*
31 660 *Microbiology*, 25, 56-66.
32 661 28. Folke, C., Carpenter, S., Walker, B., Scheffer, M., Elmqvist, T., Gunderson, L. *et al.*
33 662 (2004). Regime Shifts, Resilience, and Biodiversity in Ecosystem Management. *Annual*
34 663 *Review of Ecology, Evolution, and Systematics*, 35, 557-581.
35 664 29. Fukami, T. (2015). Historical Contingency in Community Assembly: Integrating Niches,
36 665 Species Pools, and Priority Effects. *Annual Review of Ecology, Evolution, and*
37 666 *Systematics*, 46, 1-23.
38 667 30. Fukami, T., Dickie, I.A., Paula Wilkie, J., Paulus, B.C., Park, D., Roberts, A. *et al.*
39 668 (2010). Assembly history dictates ecosystem functioning: evidence from wood
40 669 decomposer communities. *Ecology Letters*, 13, 675-684.
41 670 31. Fukami, T., Martijn Bezemer, T., Mortimer, S.R. & van der Putten, W.H. (2005). Species
42 671 divergence and trait convergence in experimental plant community assembly. *Ecology*
43 672 *Letters*, 8, 1283-1290.
44 673 32. Garnier, E., Cortez, J., Billès, G., Navas, M.-L., Roumet, C., Debussche, M. *et al.* (2004).
45 674 Plant functional markers capture ecosystem properties during secondary succession.
46 675 *Ecology*, 85, 2630-2637.
47
48
49
50
51
52
53
54
55
56
57
58
59
60

- 676 33. Gasse, F., Juggins, S. & Khelifa, L.B. (1995). Diatom-based transfer functions for
677 inferring past hydrochemical characteristics of African lakes. *Palaeogeography,*
678 *Palaeoclimatology, Palaeoecology*, 117, 31-54.
- 679 34. Gottwald, G.A. & Melbourne, I. (2004). A new test for chaos in deterministic systems.
680 *Proceedings of the Royal Society of London A: Mathematical, Physical and Engineering*
681 *Sciences*, 460, 603-611.
- 682 35. Guiot, J., Pons, A., de Beaulieu, J.L. & Reille, M. (1989). A 140,000-year continental
683 climate reconstruction from two European pollen records. *Nature*, 338, 309-313.
- 684 36. Guisan, A. & Thuiller, W. (2005). Predicting species distribution: offering more than
685 simple habitat models. *Ecology Letters*, 8, 993-1009.
- 686 37. Hampe, A. & Petit, R.J. (2005). Conserving biodiversity under climate change: the rear
687 edge matters. *Ecology Letters*, 8, 461-467.
- 688 38. Harbert, R.S. & Nixon, K.C. (2015). Climate reconstruction analysis using coexistence
689 likelihood estimation (CRACLE): A method for the estimation of climate using
690 vegetation. *American Journal of Botany*, 102, 1277-1289.
- 691 39. Hargreaves, A.L., Samis, K.E. & Eckert, C.G. (2014). Are Species Range Limits Simply
692 Niche Limits Writ Large? A Review of Transplant Experiments beyond the Range. *The*
693 *American Naturalist*, 183, 157-173.
- 694 40. Harrison, S. (1999). Local and regional diversity in a patchy landscape: native, alien, and
695 endemic herbs on serpentine. *Ecology*, 80, 70-80.
- 696 41. Hoffmann, A.A. & Sgro, C.M. (2011). Climate change and evolutionary adaptation.
697 *Nature*, 470, 479-485.
- 698 42. Holt, R.D. (2009). Bringing the Hutchinsonian niche into the 21st century: Ecological
699 and evolutionary perspectives. *Proceedings of the National Academy of Sciences*, 106,
700 19659-19665.
- 701 43. Holyoak, M., Leibold, M.A. & Holt, R.D. (2005). *Metacommunities: spatial dynamics*
702 *and ecological communities*. University of Chicago Press.
- 703 44. Jackson, S.T. & Overpeck, J.T. (2000). Responses of plant populations and communities
704 to environmental changes of the late Quaternary. *Paleobiology*, 26, 194-220.
- 705 45. Jackson, S.T. & Sax, D.F. (2010). Balancing biodiversity in a changing environment:
706 extinction debt, immigration credit and species turnover. *Trends in Ecology & Evolution*,
707 25, 153-160.
- 708 46. Jordan, G.J. (2011). A critical framework for the assessment of biological palaeoproxies:
709 predicting past climate and levels of atmospheric CO₂ from fossil leaves. *New*
710 *Phytologist*, 192, 29-44.
- 711 47. Katok, A. & Hasselblatt, B. (1997). *Introduction to the modern theory of dynamical*
712 *systems*. Cambridge University Press, Cambridge.
- 713 48. Keane, R.M. & Crawley, M.J. (2002). Exotic plant invasions and the enemy release
714 hypothesis. *Trends in Ecology & Evolution*, 17, 164-170.
- 715 49. Kimberley, A., Blackburn, G.A., Whyatt, J.D. & Smart, S.M. (2016). How well is current
716 plant trait composition predicted by modern and historical forest spatial configuration?
717 *Ecography*, 39, 67-76.
- 718 50. Kühl, N., Gebhardt, C., Litt, T. & Hense, A. (2002). Probability Density Functions as
719 Botanical-Climatological Transfer Functions for Climate Reconstruction. *Quaternary*
720 *Research*, 58, 381-392.

1
2
3 721 51. Kuneš, P., Odgaard, B.V. & Gaillard, M.-J. (2011). Soil phosphorus as a control of
4 722 productivity and openness in temperate interglacial forest ecosystems. *Journal of*
5 723 *Biogeography*, 38, 2150-2164.
6
7 724 52. La Sorte, F.A. & Jetz, W. (2012). Tracking of climatic niche boundaries under recent
8 725 climate change. *Journal of Animal Ecology*, 81, 914-925.
9 726 53. Lee-Yaw, J.A., Kharouba, H.M., Bontrager, M., Mahony, C., Csergő, A.M., Noreen,
10 727 A.M.E. *et al.* (2016). A synthesis of transplant experiments and ecological niche models
11 728 suggests that range limits are often niche limits. *Ecology Letters*, 19, 710-722.
12 729 54. Lenoir, J., Graae, B.J., Aarrestad, P.A., Alsos, I.G., Armbruster, W.S., Austrheim, G. *et*
13 730 *al.* (2013). Local temperatures inferred from plant communities suggest strong spatial
14 731 buffering of climate warming across Northern Europe. *Global Change Biology*, 19, 1470-
15 732 1481.
16
17 733 55. Lorenz, D.J., Nieto-Lugilde, D., Blois, J.L., Fitzpatrick, M.C. & Williams, J.W. (2016).
18 734 Downscaled and debiased climate simulations for North America from 21,000 years ago
19 735 to 2100AD. *Scientific Data*, 3, 160048
20 736 56. Lorenz, E.N. (1995). *The essence of chaos*. University of Washington Press, Seattle.
21 737 57. Maguire, K.C., Nieto-Lugilde, D., Blois, J.L., Fitzpatrick, M.C., Williams, J.W., Ferrier,
22 738 S. *et al.* (2016). Controlled comparison of species- and community-level models across
23 739 novel climates and communities. *Proceedings of the Royal Society of London B:*
24 740 *Biological Sciences*, 283.
25
26 741 58. Maiorano, L., Cheddadi, R., Zimmermann, N.E., Pellissier, L., Petitpierre, B., Pottier, J.
27 742 *et al.* (2013). Building the niche through time: using 13,000 years of data to predict the
28 743 effects of climate change on three tree species in Europe. *Global Ecology and*
29 744 *Biogeography*, 22, 302-317.
30
31 745 59. Mason, S. (2000). Fire and Mesolithic subsistence—managing oaks for acorns in
32 746 northwest Europe? *Palaeogeography, Palaeoclimatology, Palaeoecology*, 164, 139-150.
33 747 60. Mitton, J.B. & Grant, M.C. (1996). Genetic Variation and the Natural History of Quaking
34 748 Aspen. *BioScience*, 46, 25-31.
35
36 749 61. Morueta-Holme, N., Engemann, K., Sandoval-Acuña, P., Jonas, J.D., Segnitz, R.M. &
37 750 Svenning, J.-C. (2015). Strong upslope shifts in Chimborazo's vegetation over two
38 751 centuries since Humboldt. *Proceedings of the National Academy of Sciences*, 112, 12741-
39 752 12745.
40
41 753 62. Mosbrugger, V. & Utescher, T. (1997). The coexistence approach — a method for
42 754 quantitative reconstructions of Tertiary terrestrial palaeoclimate data using plant fossils.
43 755 *Palaeogeography, Palaeoclimatology, Palaeoecology*, 134, 61-86.
44 756 63. Nicotra, A.B., Atkin, O.K., Bonser, S.P., Davidson, A.M., Finnegan, E.J., Mathesius, U.
45 757 *et al.* (2010). Plant phenotypic plasticity in a changing climate. *Trends in plant science*,
46 758 15, 684-692.
47
48 759 64. Nogué, S., de Nascimento, L., Fernández-Palacios, J.M., Whittaker, R.J. & Willis, K.J.
49 760 (2013). The ancient forests of La Gomera, Canary Islands, and their sensitivity to
50 761 environmental change. *Journal of Ecology*, 101, 368-377.
51
52 762 65. Normand, S., Ricklefs, R.E., Skov, F., Bladt, J., Tackenberg, O. & Svenning, J.-C.
53 763 (2011). Postglacial migration supplements climate in determining plant species ranges in
54 764 Europe. *Proceedings of the Royal Society B: Biological Sciences*, 278, 3644-3653.
55 765 66. Nowacki, G.J. & Abrams, M.D. (2015). Is climate an important driver of post-European
56 766 vegetation change in the Eastern United States? *Global Change Biology*, 21, 314-334.
57
58
59
60

- 767 67. Petchey, O.L., McPhearson, P.T., Casey, T.M. & Morin, P.J. (1999). Environmental
768 warming alters food-web structure and ecosystem function. *Nature*, 402, 69-72.
- 769 68. Petchey, O.L., Pontarp, M., Massie, T.M., Kéfi, S., Ozgul, A., Weilenmann, M. *et al.*
770 (2015). The ecological forecast horizon, and examples of its uses and determinants.
771 *Ecology Letters*, 18, 597-611.
- 772 69. Peterson, A.T. (2011). *Ecological niches and geographic distributions (MPB-49)*.
773 Princeton University Press, Princeton.
- 774 70. Pross, J., Klotz, S. & Mosbrugger, V. (2000). Reconstructing palaeotemperatures for the
775 Early and Middle Pleistocene using the mutual climatic range method based on plant
776 fossils. *Quaternary Science Reviews*, 19, 1785-1799.
- 777 71. Sastry, S.S. (2013). *Nonlinear systems: analysis, stability, and control*. Springer Science
778 & Business Media.
- 779 72. Scheffer, M. & Carpenter, S.R. (2003). Catastrophic regime shifts in ecosystems: linking
780 theory to observation. *Trends in Ecology & Evolution*, 18, 648-656.
- 781 73. Schöb, C., Butterfield, B.J. & Pugnaire, F.I. (2012). Foundation species influence trait-
782 based community assembly. *New Phytologist*, 196, 824-834.
- 783 74. Seddon, A.W., Macias-Fauria, M., Long, P.R., Benz, D. & Willis, K.J. (2016). Sensitivity
784 of global terrestrial ecosystems to climate variability. *Nature*, 531, 229-232.
- 785 75. Seddon, A.W., Macias-Fauria, M. & Willis, K.J. (2015). Climate and abrupt vegetation
786 change in Northern Europe since the last deglaciation. *The Holocene*, 25, 25-36.
- 787 76. Shuman, B.N., Newby, P. & Donnelly, J.P. (2009). Abrupt climate change as an
788 important agent of ecological change in the Northeast U.S. throughout the past 15,000
789 years. *Quaternary Science Reviews*, 28, 1693-1709.
- 790 77. Silvertown, J., Dodd, M.E., Gowing, D.J.G. & Mountford, J.O. (1999). Hydrologically
791 defined niches reveal a basis for species richness in plant communities. *Nature*, 400, 61-
792 63.
- 793 78. Silvertown, J., Poulton, P., Johnston, E., Edwards, G., Heard, M. & Biss, P.M. (2006).
794 The Park Grass Experiment 1856–2006: its contribution to ecology. *Journal of Ecology*,
795 94, 801-814.
- 796 79. Singer, A., Johst, K., Banitz, T., Fowler, M.S., Groeneveld, J., Gutiérrez, A.G. *et al.*
797 (2016). Community dynamics under environmental change: How can next generation
798 mechanistic models improve projections of species distributions? *Ecological Modelling*,
799 326, 63-74.
- 800 80. Soberón, J. & Nakamura, M. (2009). Niches and distributional areas: Concepts, methods,
801 and assumptions. *Proceedings of the National Academy of Sciences*, 106, 19644-19650.
- 802 81. Sugihara, G., May, R., Ye, H., Hsieh, C.-h., Deyle, E., Fogarty, M. *et al.* (2012).
803 Detecting Causality in Complex Ecosystems. *Science*, 338, 496-500.
- 804 82. Svenning, J.-C., Eiserhardt, W.L., Normand, S., Ordonez, A. & Sandel, B. (2015). The
805 Influence of Paleoclimate on Present-Day Patterns in Biodiversity and Ecosystems.
806 *Annual Review of Ecology, Evolution, and Systematics*, 46, 551-572.
- 807 83. Svenning, J.-C. & Sandel, B. (2013). Disequilibrium vegetation dynamics under future
808 climate change. *American Journal of Botany*, 100, 1266-1286.
- 809 84. Svenning, J.-C. & Skov, F. (2007). Could the tree diversity pattern in Europe be
810 generated by postglacial dispersal limitation? *Ecology Letters*, 10, 453-460.
- 811 85. ter Braak, C.J.F. & Prentice, I.C. (1988). A Theory of Gradient Analysis. *Advances in*
812 *Ecological Research*, 18, 271-317.

1
2
3 813 86. van der Sande, M.T., Arets, E.J.M.M., Peña-Claros, M., de Avila, A.L., Roopsind, A.,
4 814 Mazzei, L. *et al.* (2016). Old-growth Neotropical forests are shifting in species and trait
5 815 composition. *Ecological Monographs*, 86, 228-243.
6 816 87. Veloz, S.D., Williams, J.W., Blois, J.L., He, F., Otto-Bliesner, B. & Liu, Z. (2012). No-
7 817 analog climates and shifting realized niches during the late quaternary: implications for
8 818 21st-century predictions by species distribution models. *Global Change Biology*, 18,
9 819 1698-1713.
10 820 88. von Humboldt, A. & Bonpland, A. (1807 (tr. 2009)). *Essay on the Geography of Plants*.
11 821 (ed. Jackson, ST). University of Chicago Press Paris.
12 822 89. Vucetich, J. & Peterson, R. (2012). The population biology of Isle Royale wolves and
13 823 moose: an overview. Available at: <http://www.isleroyalewolf.org>.
14 824 90. Webb, T. (1986). Is vegetation in equilibrium with climate? How to interpret late-
15 825 Quaternary pollen data. *Vegetatio*, 67, 75-91.
16 826 91. Whittaker, R.H. (1967). Gradient analysis of vegetation. *Biological Reviews*, 42, 207-
17 827 264.
18 828 92. Williams, J.W., Blois, J.L. & Shuman, B.N. (2011). Extrinsic and intrinsic forcing of
19 829 abrupt ecological change: case studies from the late Quaternary. *Journal of Ecology*, 99,
20 830 664-677.
21 831 93. Willis, K.J., Bennett, K.D., Burrough, S.L., Macias-Fauria, M. & Tovar, C. (2013).
22 832 Determining the response of African biota to climate change: using the past to model the
23 833 future. *Philosophical Transactions of the Royal Society of London B: Biological*
24 834 *Sciences*, 368.
25 835 94. Wisz, M.S., Pottier, J., Kissling, W.D., Pellissier, L., Lenoir, J., Damgaard, C.F. *et al.*
26 836 (2013). The role of biotic interactions in shaping distributions and realised assemblages
27 837 of species: implications for species distribution modelling. *Biological Reviews*, 88, 15-30.
28 838 95. Ye, H., Beamish, R.J., Glaser, S.M., Grant, S.C.H., Hsieh, C.-h., Richards, L.J. *et al.*
29 839 (2015). Equation-free mechanistic ecosystem forecasting using empirical dynamic
30 840 modeling. *Proceedings of the National Academy of Sciences*, 112, E1569-E1576.
31 841 96. Zurell, D., Thuiller, W., Pagel, J., S Cabral, J., Münkemüller, T., Gravel, D. *et al.* (2016).
32 842 Benchmarking novel approaches for modelling species range dynamics. *Global Change*
33 843 *Biology*, 22, 2651-2664.
34 844
35
36
37
38
39
40
41
42
43
44
45
46
47
48
49
50
51
52
53
54
55
56
57
58
59
60

Box 1. Definitions of lag statistics for community dynamics

Consider a community containing a set of $\{i\} \in (1, k)$ species at time t . Each resident species i has a fundamental niche function that can be described by a relative fitness over a given niche axis. Suppose that each of these niche functions has a modal value of $N_i(t)$.

The location of the community has an **observed climate** $F(t)$. The **inferred climate** of the community also can be defined as the mean of the niche optima of all species (**Fig. 1**):

$$(B1-1) \quad C(t) = E[N_i(t)]$$

More sophisticated definitions (e.g. abundance-weighted means or medians across species) are possible and potentially more useful in low-richness communities.

We can also define a measure of uncertainty in the inferred climate, $\sigma(t)$, as the standard deviation of the modal niche values:

$$(B1-2) \quad \sigma(t) = \sqrt{E[(N_i(t) - C(t))^2]}$$

If a community is comprised of species with similar $N_i(t)$ values, then $\sigma(t)$ is close to zero; alternatively, if species have a wide range of $N_i(t)$ values, then $\sigma(t)$ is large. Large values of $\sigma(t)$ can also represent community lag resulting from differences in species responses to changing climatic conditions, but we primarily consider them as uncertainties in the context of empirical data.

The **community climate lag** can be defined as the difference between the inferred climate and observed climate. It can be calculated at any given time t :

$$(B1-3) \quad \Lambda(t) = C(t) - F(t)$$

Because of linearity, the standard deviation (uncertainty) of $\Lambda(t)$ is also equal to $\sigma(t)$.

The **mean absolute deviation** can be defined as:

1
2
3
4
5
6
7
8
9
10
11
12
13
14
15
16
17
18
19
20
21
22
23
24
25
26
27
28
29
30
31
32
33
34
35
36
37
38
39
40
41
42
43
44
45
46
47
48
49
50
51
52
53
54
55
56
57
58
59
60

(B1-4)
$$\overline{|\Lambda|} = \frac{1}{t_{\max}} \int_0^{t_{\max}} |\Lambda(t)| dt$$

where generally the statistic would be calculated for $t_{\max} \rightarrow \infty$.

The **maximum state number** can be defined as the largest number of real values of C corresponding to any of the realized values of F . Let g be the implicit constraint equation defining the relationship between F and C , i.e. $g(C,F)=0$. Then n is the maximum cardinality of the set of real roots of g for each value of F :

(B1-5)
$$n = \max_F \left| \{C \in \mathfrak{R} : g(C,F) = 0\} \right|$$

There are several ways to calculate n . If $g(C,F)=0$ is a polynomial in C , then an exact value for n can easily be obtained using Sturm's theorem for counting distinct real roots (Dorrie & Antin 1965). In the more general case, if $g(C,F)=0$ is transcendental in C , then g can be approximated to arbitrary accuracy by Chebyshev polynomials, with real roots counted using companion matrix eigenvalue methods (Boyd 2013).

It is also possible to obtain an upper bound on the maximum state number. As we prove in **Supplementary Text S1**, if F and C are both periodic in time, then the maximum state number is always finite, with

(B1-6)
$$n \leq kb.$$

where k is the number of times F folds over itself in one period in the F - C plane, and b is the relative periodicity of F relative to C . The analytical bound essentially reflects how synchronized the observed and inferred climates are. Thus, even with *stable* dynamics characterized by periodic orbits, predictability of the community can vary strongly. Moreover, a simple functional form for $F(t)$ does not imply simple predictability in the inferred climate. The state number, which can be understood as a metric that characterizes the *complexity* of those

889 dynamics, is a valuable measure for predictability and the diversity of community responses
890 possible.

For Review Only

1
2
3
4
5
6
7
8
9
10
11
12
13
14
15
16
17
18
19
20
21
22
23
24
25
26
27
28
29
30
31
32
33
34
35
36
37
38
39
40
41
42
43
44
45
46
47
48
49
50
51
52
53
54
55
56
57
58
59
60

Box 2. A simple model of community dynamics

We propose an ordinary differential equation model for the dynamics of a community's state, $C(t)$. The model's formulation is general, but is operationalized here with linear functions to demonstrate the range of complex behavior that can arise from simple model structure.

(B2-1)
$$\frac{dC(t)}{dt} = -c_T T[\tau(t)] - c_R R[\rho(t)]$$

where $T[\tau(t)]$ is a function describing how the community tracks a change $\tau(t)$ in its state relative to the observed climate at time t and $R[\rho(t)]$ is a function describing how the community resists a change $\rho(t)$ in its state at time t relative to a past observed climate. The coefficients $c_R \geq 0$ and $c_T \geq 0$ determine the relative importance of each effect. This model describes a forced delay differential equation, whose general properties and solutions have been explored in the mathematics and control theory literature (Sastry 2013).

The size of the tracking change, $\tau(t)$, can be defined as the linear difference between the observed climate and the community composition at time t :

(B2-2)
$$\tau(t) = C(t) - F(t) = \Lambda(t)$$

We consider two possibilities for the resistance change, $\rho(t)$. One is to define resistance by the linear difference between the community composition at time t and the community composition based on a time delay, Δt :

(B2-3)
$$\rho(t) = C(t) - C(t - \Delta t)$$

This models a scenario where the amount of restorative force is proportional to the difference between the community's past and present state, so that the system tends toward a past state (e.g.

maintenance of an already-established forest type). Another is to use the difference between the community state at time $t - \Delta t$ and a optimal state C_0 .

$$(B2-4) \quad \rho(t) = C(t - \Delta t) - C_0,$$

which models a scenario where the system tends toward a fixed climate-independent optimum.

A simple proposal for the tracking function is a linear function:

$$(B2-5) \quad T(\tau) = \tau.$$

where the response of a community to climate is directly proportional to the lag at that time.

Similarly, a simple resistance function can be proposed with a linear response, for

example

$$(B2-6) \quad R(\rho) = \rho$$

or with a nonlinear response, as

$$(B2-7) \quad R(\rho) = \rho^3$$

Both resistance functions are odd and therefore yield responses that are restorative, in that they try to maintain the system in its current state. Another proposal is a nonlinear restorative function with multiple basins of attraction:

$$(B2-8) \quad R(\rho) = \sin(\rho) \cdot \exp(-\rho^2)$$

This equation describes a situation where small to medium changes in system state lead to increasingly strong restorative responses, but where large changes lead to non-restorative responses.

The model also depends on the temporal trajectory of the observed climate $F(t)$. Here, we consider two simple example cases for climate change: a linearly increasing forcing with rate γ :

$$(B2-9) \quad F_{linear}(t) = \gamma t$$

and a periodic forcing with angular frequency ω :

(B2-10) $F_{periodic}(t) = \sin(\omega t)$

First, consider the linear forcing. In the case that $c_R=0$ (no resistance effects), **Equation B2-1** reduces to

(B2-11) $\frac{dC(t)}{dt} = -c_T(C(t) - \gamma t)$

and has solution when $C(0)=0$ of

(B2-12) $C(t) = \gamma \left(t + \frac{e^{-c_T t} - 1}{c_T} \right) = F(t) - \frac{\gamma}{c_T} (1 - e^{-c_T t})$

That is, the system is delayed by $\frac{\gamma}{c_T} (1 - e^{-c_T t})$. The second term rapidly decays over time, so the lag converges on a constant value as time increases. If $c_T=0$, the delay become zero. Thus, only no-lag (**Fig. 3A**) or constant-lag (**Fig. 3B**) dynamics can occur.

If instead resistance does occur ($c_R>0$), then **Equation B2-1** no longer has an exact solution. However, the system does respond with constant relationship dynamics regardless of the choice of resistance function. Indeed, for any monotonic forcing function this will be the case. For monotonic forcing, F and t are in a one-to-one relationship. Therefore, a given choice $F = F_0$ will correspond to a single time $t = t_0$. Since $C(t)$ must be a function (emerging as the solution of a differential equation), fixing $t = t_0$ fixes $C = C_0 = C(t_0)$. This implies that even though $C(t)$ is not necessarily (in fact, usually not) a monotonic function, a given F corresponds to a single C , and thus the community response diagram in the $F - C$ plane will be one-to-one, for which the state number is always $n=1$ (**Fig. 3B**). The general implication is that only constant-lag, constant-relationship, and no-lag dynamics are possible with linear climate change.

Next, consider the periodic forcing. The no-lag and constant delay hypotheses can both occur when there are no resistance effects ($c_R=0$). The system reduces to

$$(B2-13) \quad \frac{dC(t)}{dt} = -c_T (C(t) - \sin(\omega t))$$

In this case, the solution, assuming $C(0)=0$, becomes

$$(B2-14) \quad C(t) = \frac{c_T}{c_T^2 + \omega^2} \left[c_T \sin(\omega t) - \omega \sin\left(\frac{\pi}{2} - \omega t\right) + \omega e^{-c_T t} \right]$$

That is, the community response is proportional to the sum of the observed climate, a time delayed observed climate, and a transient coefficient that decays rapidly over time (**Fig. 3C**). As the parameter c_T becomes large relative to ω , $C(t)$ converges exactly on $F(t)$ and the time lag disappears. That is, when $c_R=0$, a small value of c_T corresponds to the constant-lag hypothesis, and a large value of c_T corresponds to the no-lag hypothesis.

Alternatively when resistance effects also occur ($c_R>0$), the type of dynamics depends on the size and form of the resistance. For the simple lagged resistance (**Equation B2-3**), constant-lag and alternate state dynamics can occur, but are restricted to state number $n=2$ (**Fig. 3D**). For the more complex restorative resistance change (**Equation B2-4**) and resistance functions (**Equation B2-7**), we find far more complex dynamics exhibited, including periodic states with state number $n \geq 2$ (**Fig. 3E**), as well as chaos in some parameter regimes (**Fig. 3F**).

We can also determine when (if ever) the system reaches a steady state, depending on the presence of resistance or tracking effects. As proved in **Supplementary Text S2**, we can separate the community's dynamics into transient effects and steady states (except in the case of parameters leading to chaos). In the transient state, the system takes a trajectory that is highly influenced by initial conditions that can be difficult to predict. After the system settles to a steady state, $C(t)$ becomes a periodic function, and the community response diagram follows a fixed

1
2
3 975 pattern that repeats over time. The duration of the transient increases with decreases in the ratio
4
5
6 976 $\frac{c_T}{c_R}$, i.e. as resistance effects dominate tracking effects. The previous result holds except for where
7
8
9 977 the tracking function restores toward a climate-independent state (Equation B2-4). In this case,
10
11 978 are parameter regimes where the transient grows with time, even while the community is
12
13 979 restoring toward a constant state. Thus the system never obtains a fixed pattern that repeats over
14
15
16 980 time and instead exhibits transient dynamics for all times that may have arbitrarily high n and $|\Lambda|$
17
18
19 981 .
20
21 982

For Review Only

Figures

984

Fig. 1. A) Definition of community and climate terms. A community contains a set of resident species, each described by a different realized climate niche (cyan distributions) at time t . By overlapping these niches, a climate most consistent with the occurrence of these species (blue distribution) can be inferred and summarized by its expected value, defined as the community climate, $C(t)$ (vertical blue line). The community climate may differ from the observed climate at the location of the community, $F(t)$ (vertical red line). The difference between the community climate and the observed climate is defined as the community climate lag, $\Lambda(t)$. If the community is in equilibrium with climate and there are no lags, $\Lambda(t) = 0$, or $|\Lambda(t)| > 0$ otherwise. **B)** An example of time series for $C(t)$ and $F(t)$. Values of zero are shown as a dashed horizontal line. **C)** A community response diagram is a parametric plot of time-series of $F(t)$ and $C(t)$. Data are replotted here from panel B. Values of zero are shown as dashed horizontal and vertical lines. The 1:1 no-lag expectation of $C(t) = F(t)$ is shown as a gray line.

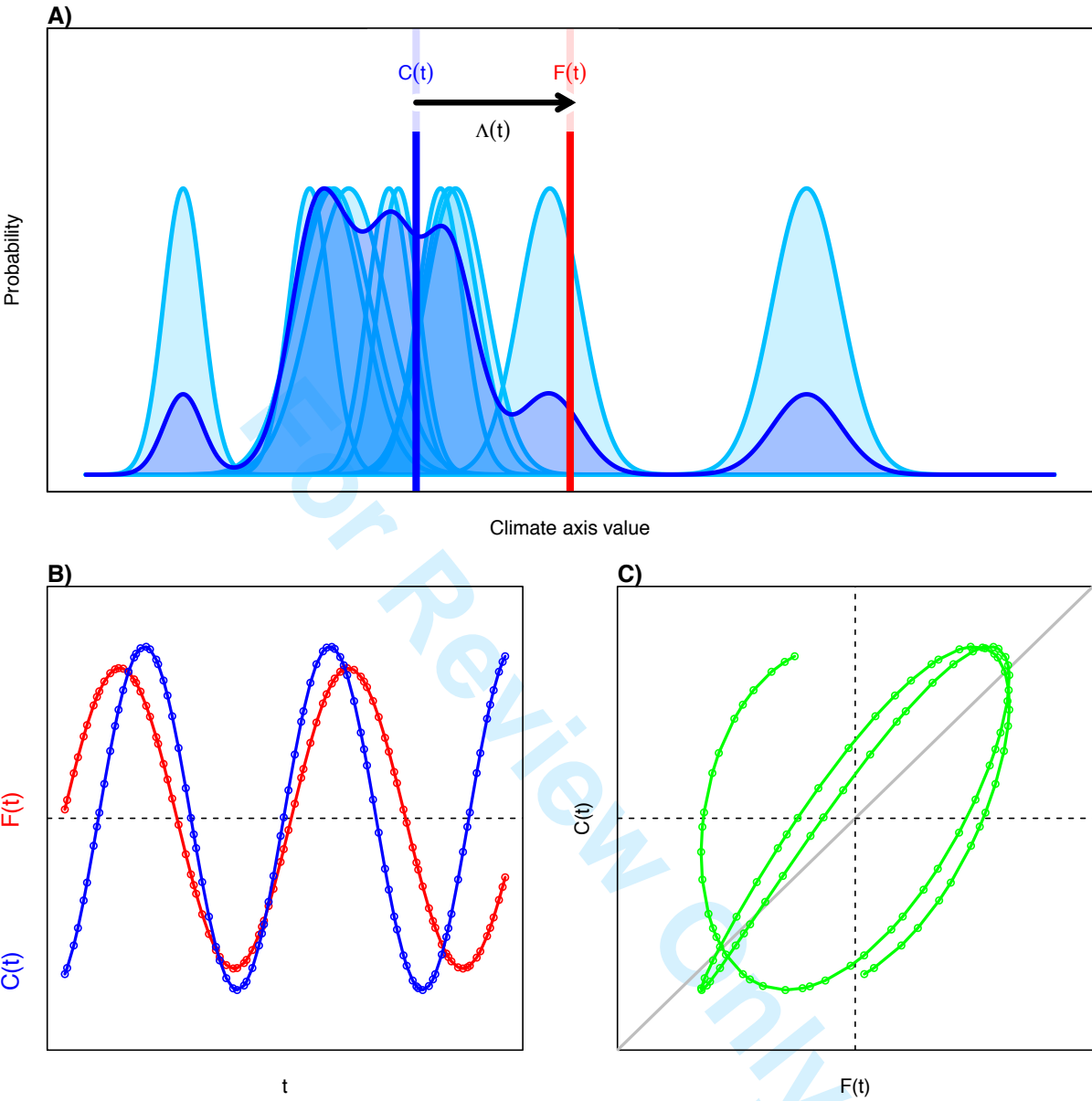
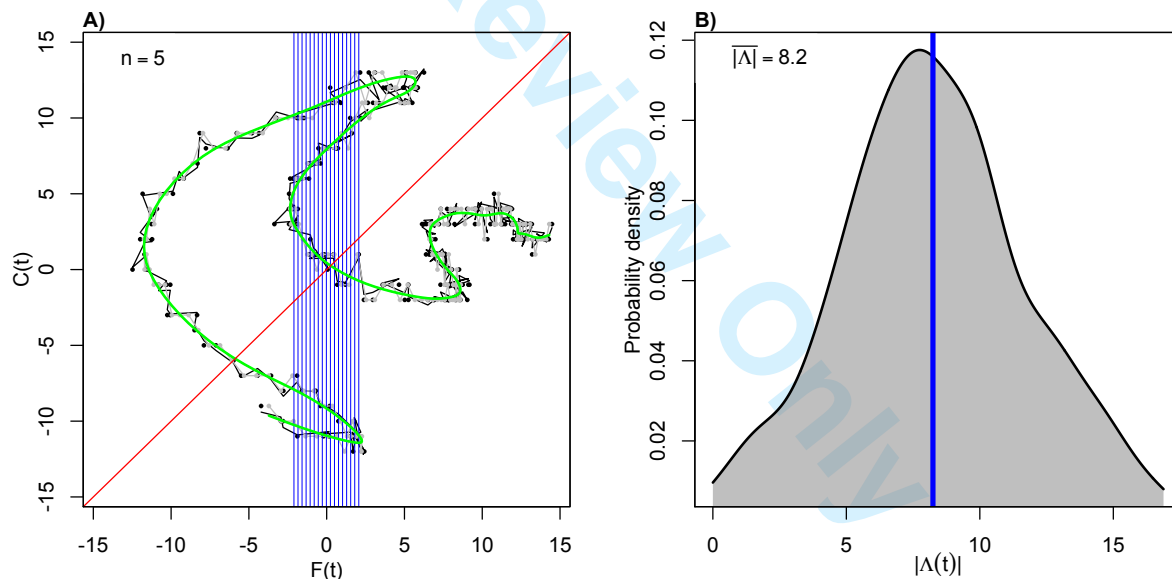


Fig. 2. Definition of community response diagram statistics using an example dataset. **A)** A community's trajectory of observed climate $F(t)$ and the community response $C(t)$ is shown for original data (black curve), coarsened data (gray curve), and coarsened and smoothed data (blue curve). The 1:1 (no lag) expectation is shown as a diagonal red line. The maximum state number, n , indicates the largest number of unique values of $C(t)$ that correspond to any coarsened value of $F(t)$. It is calculated by intersecting a vertical line with the community's trajectory at all values of $F(t)$ (vertical blue lines). **B)** The mean absolute deviation, $|\overline{\Lambda}|$, indicates the average difference between $C(t)$ and $F(t)$ across all times, with larger values indicating greater lags. The distribution of lags is shown as a gray envelope and the statistic's value is shown as a vertical blue line.



1
2
3 1011 **Fig. 3.** General classes of dynamics possible for a community's response to climate change. In
4
5
6 1012 each box, the time series shows an observed climate $F(t)$ (red lines) and a community response
7
8 1013 $C(t)$ (blue lines). Values of the state number n and the mean absolute deviation $|\overline{\Lambda}|$ are shown as
9
10
11 1014 insets for each example. **A)** No-lag dynamics occur where the community climate closely
12
13 1015 matches the observed climate. This scenario can be detected when the community response
14
15 1016 diagram matches the 1:1 line. **B)** Constant relationship dynamics occur when the community
16
17 1017 response diagram is a function, i.e. has a unique value of $C(t)$ for every value of $F(t)$. **C)**
18
19
20 1018 Constant delay dynamics occur when the community climate follows the observed climate with a
21
22 1019 fixed time delay. This scenario cannot be detected for a linear climate change but appears as a
23
24 1020 single loop for a sinusoidal climate change. Transient effects can also occur producing
25
26 1021 unpredictable dynamics with high n . **D)** Memory effects occur when the community climate
27
28 1022 follows the observed climate with a variable delay and magnitude. This scenario can be detected
29
30 1023 via the presence of one or more crossing-back events that can also form loops when $F(t)$ is
31
32 1024 periodic. **E)** Alternate unstable states occur when the community shows memory effects with
33
34 1025 multiple stacked loops, such that the state number is always greater than two. **F)** Unpredictable
35
36 1026 dynamics can occur when n becomes infinite. Memory effects occur in this scenario as well. A
37
38 1027 scenario is shown here for chaos. **G)** Unpredictable dynamics can also occur when the
39
40 1028 community response is uncorrelated with the observed climate, e.g. because of stochastic
41
42 1029 dynamics. All trajectories were generated from the model in **Box 2** using parameter
43
44 1030 combinations described **Table S1**.
45
46
47
48
49
50
51
52
53
54
55
56
57
58
59
60

